Large-scale vertical vorticity generated by two crossing surface waves

Vladimir M. Parfenyev* and Sergey S. Vergeles
Landau Institute for Theoretical Physics, Russian Academy of Sciences, 1-A Akademika Semenova av., 142432 Chernogolovka, Russia
and National Research University Higher School of Economics, Faculty of Physics, Myasnitskaya 20, 101000 Moscow, Russia

(Received 14 May 2020; accepted 14 September 2020; published 30 September 2020)

We demonstrate that two surface waves propagating at a small angle 2θ to each other generate large-scale (compared to the wavelength) vertical vorticity owing to hydrodynamic nonlinearity in a viscous fluid. The horizontal geometric structure of the induced flow coincides with the structure of the Stokes drift in an ideal fluid, but its steady-state amplitude is larger and it penetrates deeper into the fluid volume as compared to the Stokes drift. In an unbounded fluid, the steady-state amplitude and penetration depth are increased by the factor of $1/\sin\theta$ and the evolution time of the induced flow can be estimated as $1/(4\nu k^2 \sin^2\theta)$, where ν is the fluid kinematic viscosity and k is the wave number. Also, we study how the finite depth of the fluid and a thin insoluble liquid film that possibly covers the fluid surface due to contamination effect the generation of large-scale vorticity and discuss the physical consequences of this phenomenon in the context of recent experiments.

DOI: 10.1103/PhysRevFluids.5.094702

I. INTRODUCTION

Recent experiments have shown that surface waves generate intense solenoidal currents on the fluid surface [1–8]. The explanation of how the wave oscillations excite the slow horizontal flows has a long history dating back to Longuet-Higgins' seminal paper [9]. At the initial stage, the generation is related to the fluid viscosity (which is relevant in a narrow layer near the fluid surface and the boundaries) and nonlinearity of surface waves. The fluid viscosity causes attenuation of the wave motion and its momentum is transferred to slow currents by the action of the virtual wave stress [10]. Subsequent studies proposed the description in Lagrangian coordinates, investigated the role of Coriolis force, and analyzed nonstationary regimes; see [11–17] and references therein. The next step was made in the work in [18], which generalizes the pioneering results obtained for a plane wave to the case of surface waves propagating in arbitrary directions. Later, a particular case of slow currents generated by orthogonal surface waves has been analyzed in detail [7,19]. The resulting flow has the form of a regular lattice of vortices rotating in opposite directions, with the size of each vortex equal to half the wavelength.

At large Reynolds numbers, the regular vortex lattice is distorted after some time, which is accompanied by the appearance of vortex flows with larger scales. This phenomenon was observed in experiments of two different types. In the first case, surface waves were excited due to Faraday instability and the solenoidal currents became chaotic, showing an unexpected resemblance to two-dimensional turbulence [1], even when the fluid depth exceeded the wavelength [2,3]. The surface elevation had a narrow peaked wave-number spectrum, while the horizontal surface flow demonstrated a wide Kolmogorov $k^{-5/3}$ spectrum. As an explanation, it was proposed that surface

*parfenius@gmail.com

waves generate horizontal solenoidal currents with a size of the order of the wavelength, and then the energy is redistributed to larger scales due to the inverse energy cascade [2,3], which was confirmed by the measurement of the third-order structure function. Despite this, the mechanism of the upscale energy transfer has remained unclear, because the theory of the inverse energy cascade was developed only for two-dimensional (2D) and quasi-2D systems [20], and the considered case is essentially three dimensional. In addition, the numerical analysis shows that, with such a ratio between the fluid thickness and the pumping scale, the inverse energy cascade is not realized [21–23].

In experiments of the second type [5,7], the wave motion was excited by orthogonal plungers, partially submerged into the fluid and performing monochromatic vertical oscillations. The resulting horizontal flow had the form of a regular vortex lattice and, over time, large-scale vortices with a size of the order of the system size appeared on its background. According to the measured spectrum of the horizontal flow [5], vortices of intermediate scales were not formed. Therefore, the generation of large-scale vortices in this case cannot be explained by the inverse energy cascade and, to our knowledge, no other explanation was offered. Note that a further increase in the Reynolds number leads to the generation of surface waves with other frequencies due to four-wave interactions, which significantly complicates the fluid motion [24].

Here we demonstrate that monochromatic surface waves can directly excite a large-scale horizontal flow due to hydrodynamic nonlinearity if they propagate at a small angle to each other. In the case of Faraday instability, when the threshold is significantly exceeded, several modes are excited simultaneously, which correspond to waves propagating in different directions. As for experiments, where the waves were excited by oscillating plungers, we believe that they can also excite wave modes having a nonzero component of the wave vector in the direction along the plunger. The interaction between these modes and waves propagating strictly perpendicular to the plungers leads to the generation of large-scale solenoidal surface currents. A detailed description of these currents (including their evolution over time) provided below will allow testing this hypothesis experimentally. Qualitative prediction is that, to observe such flows, it is sufficient to excite surface waves with one plunger.

Briefly summarizing results, we found that, in an unbounded fluid, the horizontal size and penetration depth of the large-scale current are equal to $L = 1/(2k \sin\theta)$, and its steady-state vertical vorticity on the fluid surface can be estimated as $\Omega_E \sim \omega k^2 H_1 H_2$. Here ω is the wave frequency, k is the wave number, H_1 and H_2 are the wave elevation amplitudes, and 2θ is the angle between waves. The kinematic viscosity ν of a fluid does not enter in these expressions; however, it determines the evolution time $T_E = L^2/\nu$ of the large-scale flow. The depth of fluid d begins to play a noticeable role if it becomes comparable to or less than L. Additional bottom friction causes a decrease in the steady-state amplitude of horizontal solenoidal flow on the surface by a factor of $\tanh(d/L)$ and also accelerates its temporal evolution. If a thin insoluble liquid film is present on the fluid surface (e.g., due to contamination [7,25]), then it can significantly increase the vertical vorticity Ω_E compared to the free surface case, provided that the wave amplitudes remain unchanged.

At last, we would like to note that the considered phenomenon is a special case of steady streaming [26], which corresponds to nonzero mean current arising from the time average of a fluctuating flow. Other well-known examples of steady streaming are acoustic streaming [27] and viscous streaming [28]. In all these cases, the steady current results from the action of Reynolds stress in a thin viscous sublayer near the boundaries or near the surface. A characteristic feature of such currents is that they penetrate far beyond the viscous sublayer, and their amplitudes do not depend on the fluid viscosity (but there are exceptions, for example, in our case, if the fluid surface is covered with a film). Read more about the similarity of these flows in the review article in [26].

II. RESULTS

Let us consider two propagating waves excited on the surface of an incompressible viscous fluid. We assume that Z axis is directed vertically, opposite to the gravitational acceleration, and that the undisturbed fluid surface (without the wave motion) coincides with plane $z = 0$. The horizontal extent is unlimited and the surface elevation is equal to

$$h(t, x, y) = H_1 \cos(\omega t - kx \sin\theta - ky \cos\theta) + H_2 \cos(\omega t + kx \sin\theta - ky \cos\theta), \tag{1}$$

where ω is the wave frequency, k is the wave number, H_1 and H_2 are the wave elevation amplitudes, and 2θ is the angle between waves. The deep-water assumption is implied, i.e., the fluid depth $d \gg 1/k$, we assume that the wave steepness is small, $|\nabla h| \ll 1$, and the kinematic viscosity ν of fluid is weak, $\gamma = \sqrt{\nu k^2/\omega} \ll 1$. As it will be shown, the nonlinear interaction between these waves leads to the generation of slow large-scale horizontal solenoidal current. We neglect the spatial decay of wave amplitudes due to the fluid viscosity in Eq. (1), and therefore our consideration also entails the smallness of the characteristic horizontal size L of the generated current compared with the propagation length of surface waves, $kL \ll 1/\gamma^2$.

Experimentally, the horizontal currents are studied by examining the trajectories of passive particles advected by the flow [1–8]. There are Stokes and Eulerian contributions to the corresponding Lagrangian velocity averaged over fast wave oscillations, which are very different [7,9]. The first contribution is a generalization of the Stokes drift for a plane wave in an ideal fluid [29]. It is the result of nonlinear Lagrangian dynamics and it does not produce any contribution to the mean velocity of fluid in the bulk in the Eulerian description [10, Sec. 2]. In contrast, the Eulerian contribution corresponds to the mean velocity of the fluid and it arises due to fluid viscosity and hydrodynamic nonlinearity [9,10] (see also Ref. [30] for a discussion of alternative methods of description). In what follows, we will describe the horizontal currents in terms of the vertical vorticity, $\Omega = \partial_x V_y - \partial_y V_x$, where V_x and V_y are horizontal components of the time-averaged Lagrangian velocity of tracers. Thus $\Omega = \Omega_S + \Omega_E$, where Ω_S takes into account the Stokes drift contribution and Ω_E corresponds to the fluid velocity in the Eulerian description; see also Refs. [7,19]. The vertical vorticity is generated due to the interaction of noncollinear waves, and its amplitude is proportional to the product of wave amplitudes. The Stokes and Eulerian contributions to the Lagrangian velocity of tracers caused by the self-nonlinearity of a plane wave were studied previously [9,29], and they give a zero contribution to the vertical vorticity.

To find the Stokes drift contribution Ω_S to the vertical vorticity, it turns out that one should implement the same calculations as for an ideal fluid [19, Sec. V]. For surface waves defined by expression (1), we obtain

$$\Omega_S = \Lambda(x) \sin\theta \, \exp(2kz), \tag{2}$$

where $\Lambda(x) = -4H_1H_2\omega k^2 \cos^3\theta \, \sin[2kx \sin\theta]$ describes the spatial structure of Ω_S in the horizontal plane; see Fig. 1. The details of the calculations can be found in Appendix A; see also Ref. [31, Eq. (31)]. In the vertical direction, the contribution penetrates to a depth of $1/(2k)$; the maximum value is reached on the fluid surface. Thus, despite the large horizontal size $L = 1/(2k \sin\theta)$, the current remains localized near the surface. In the limiting case $\sin\theta \to 0$, one finds $\Omega_S \to 0$, i.e., the Stokes drift contribution to the vertical vorticity disappears. If the wave amplitudes change over time (for example, they decrease due to viscous damping), then the Stokes drift instantly tracks these changes. Therefore, the characteristic evolution time of Ω_S can be estimated as $T_S = 1/(4\nu k^2)$. If the size of the system is limited in the horizontal direction, as is often the case in laboratory experiments, then this time can be even shorter due to additional dissipation of the wave motion near the boundaries [7,32].

The Eulerian contribution Ω_E to the vertical vorticity is excited in the viscous sublayer near the fluid surface due to the fluid viscosity and hydrodynamic nonlinearity, and then it spreads downward in the fluid bulk due to viscous diffusion. If the Reynolds number characterizing the large-scale

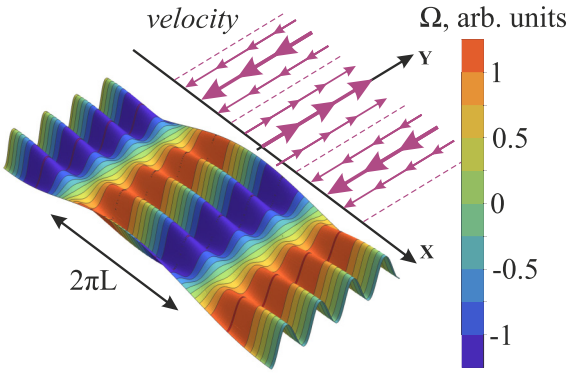

FIG. 1. Schematic of surface elevation and horizontal spatial structure $\Lambda(x)$ of the generated large-scale vorticity, which is produced by two propagating surface waves (1). The colors represent the intensity of the vertical vorticity in arbitrary units. The arrows show the corresponding velocity field. The angle between waves is equal to $2\theta = \pi/15$ and $H_1 = H_2$.

current is small, then its evolution in the fluid bulk satisfies the equation

$$\partial_t \Omega_E - \nu \nabla^2 \Omega_E = 0. \tag{3}$$

See Ref. [33, Eq. (3.20)] and Ref. [7, Eq. (7)]. The excitation process can be described in terms of the boundary condition for this equation, since the viscous sublayer has a very small thickness $\delta \sim \gamma/k$. The corresponding relation was derived for arbitrary wave motion, e.g., in Ref. [18] and Ref. [34, Eq. (15)], and for two propagating waves (1) one finds

$$\nu \partial_z \Omega_E|_{z=0} = 2\nu k \, \sin\theta \, \Lambda(x). \tag{4}$$

See also Ref. [33, Eq. (3.6)] and Ref. [35, Eq. (3)]. Another boundary condition for Eq. (3) is the disappearance of vertical vorticity at infinite depth, $\Omega_E|_{z\to-\infty} = 0$. This expression implies that the fluid depth is much greater than the penetration depth of the horizontal current Ω_E.

The stationary solution of the discussed boundary-value problem has the form

$$\Omega_E = \Lambda(x) \exp(2kz \, \sin\theta). \tag{5}$$

Compared to expression (2), the Eulerian contribution Ω_E to the vertical vorticity has the same horizontal structure $\Lambda(x)$, but its amplitude on the surface is $1/\sin\theta$ times greater and it penetrates the fluid volume much deeper, at a distance of the order of the horizontal size L. Geometrically, the flow is directed along straight strips of thickness πL and it is oppositely directed inside the neighboring strips. The corresponding velocity is equal to $V_E^y = -L\Omega_E \cot(2kx \, \sin\theta)$; see Fig. 1. The velocity distribution can be treated in terms of the well known horizontal mean drift induced by a plane wave [9] in the limit of small angle $\theta \ll 1$ as follows: the drift velocity along Y axis is increased in those regions of x where two wave amplitudes are summed producing a locally plane wave of amplitude $H_1 + H_2$ and has the minimum where the amplitudes are subtracted. The drift velocity averaged over the horizontal plane is subtracted in Fig. 1 as it is not associated with any vertical vorticity.

The characteristic time of evolution of Ω_E is determined by the fluid viscosity and we find the estimate $T_E = L^2/\nu$ from Eq. (3). At a small angle between the propagating waves, $T_E \gg T_S$, so the wave motion and the Stokes drift are established much faster than the horizontal current Ω_E. Consider the case when the fluid was initially at rest, and then the wave maker began to excite the wave motion. After a short period, the right-hand side of Eq. (4), determined by the wave motion, ceases to depend on time, and by solving Eq. (3) with the discussed boundary conditions, we obtain

the dependence of Ω_E on time and depth

$$\Omega_E(t,x,z) = \frac{\Lambda(x)}{\sqrt{\pi}} \int_0^{t/T_E} \frac{d\xi}{\sqrt{\xi}} \exp\left(-\xi - \frac{z^2}{4\xi L^2}\right). \tag{6}$$

The value of the Eulerian contribution to the vertical vorticity on the fluid surface is of particular interest because it is relatively easy to measure experimentally. By substituting $z = 0$ in expression (6), we find

$$\Omega_E(t,x,0) = \Lambda(x)\mathrm{erf}[\sqrt{t/T_E}]. \tag{7}$$

Note that at the initial stage of excitation, $t \ll T_E$, the growth is described as $\Omega_E(t,x,0) \propto \sqrt{t/T_E}$.

Similarly, we can consider the decay of horizontal slow current Ω_E after turning off the wave maker and the disappearance of the wave motion. In this case, the right-hand side in the boundary condition (4) should be equal to zero, since there are no more surface waves. As an initial condition, we assume that the vorticity distribution is described by expression (5). Then, we find

$$\Omega_E(t,x,z) = \frac{\Lambda(x)}{\pi} \int_{-\infty}^{\infty} d\xi \frac{\cos(\xi z/L)}{\xi^2+1} e^{-(\xi^2+1)t/T_E}. \tag{8}$$

By substituting $z = 0$ in expression (8), we obtain the evolution of the Eulerian contribution on the fluid surface

$$\Omega_E(t,x,0) = \Lambda(x)\mathrm{erfc}\,[\sqrt{t/T_E}]. \tag{9}$$

At the initial stage of decay, $t \ll T_E$, the dependence on time is described by a square root law $\Omega_E(t,x,0) \propto 1 - \sqrt{4t/(\pi T_E)}$, and, at large times, $t \gg T_E$, it turns into the exponential law $\Omega_E(t,x,0) \propto \sqrt{T_E/t}\exp(-t/T_E)$. Note that the performed calculations generalize the similar ones for the case of orthogonal surface waves. The details of the calculations can be found in Ref. [7, Sec. II].

Next, we consider what happens if the fluid depth d becomes comparable to or less than the horizontal size L of the generated current. Stokes drift does not change in response to the depth change, as long as the deep water approximation $kd \gg 1$ remains valid. To find the change in the Eulerian contribution to the vertical vorticity, we assume that the usual no-slip boundary condition is fulfilled on the bottom surface. Therefore, boundary-value problem (3),(4) needs to be supplemented with the condition $\Omega_E|_{z=-d} = 0$. In this case, the stationary solution has the form

$$\Omega_E = \Lambda(x)\frac{\sinh\left[(z+d)/L\right]}{\cosh\left(d/L\right)}. \tag{10}$$

The amplitude of horizontal current decreases in comparison with expression (5) due to friction against the bottom. In particular, the surface flow becomes weaker by a factor $\tanh(d/L)$.

Figure 2(a) shows the development of horizontal current Ω_E on the surface over time at various fluid depths obtained by numerical solution of the corresponding boundary-value problems. At small times $t \ll d^2/\nu$, the presence of the bottom does not have any effect and the solution is described by expression (7). At large times $t \gg \min(T_E, d^2/\nu)$, the solution reaches a stationary value determined by expression (10). Note that for a small depth $d \ll L$ the stationary solution is reached faster compared to the unbounded fluid. Analytical analysis of the problem supporting these results can be found in Appendix B.

In the same way, we can consider the attenuation of the stationary solution (10), after switching off the wave maker at $t = 0$, accompanied by fast decay of the wave motion due to the fluid viscosity. At large times $t \gg d^2/\nu$, we obtain the exponential asymptotic (see Appendix C)

$$\Omega_E(t,x,z) \to \Lambda(x)\sin\left[\frac{\pi}{2}\left(1+\frac{z}{d}\right)\right]\frac{\exp\left(-\alpha t/T_E\right)}{\alpha \cdot d/(2L)}. \tag{11}$$

The factor $\alpha = 1 + \pi^2 L^2/(4d^2)$ describes the increase in the decay rate of Ω_E compared with the case of unbounded fluid due to additional dissipation near the bottom. At the same time for $t \ll$

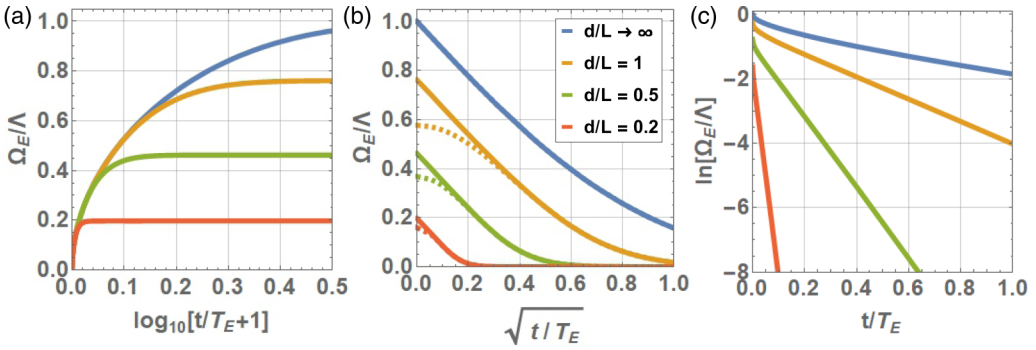

FIG. 2. Formation (a) and decay (b), (c) of the horizontal current Ω_E on the surface $z = 0$ at various fluid depths (numerical solution). The curves for unlimited depth correspond to expressions (7) and (9). Asymptotic values at large times for formation process and initial values for decay process are determined by relation (10). Dashed lines show asymptotic behavior (11). (b) illustrates that the decay rate of the vertical vorticity on the fluid surface does not depend on the fluid depth at small times $t \ll d^2/\nu$, see Eq. (12), and (c) shows the exponential law of decay at large times $t \gg d^2/\nu$: see Eq. (11).

d^2/ν, the decay rate of the vertical vorticity on the fluid surface does not depend on the fluid depth,

$$\frac{d\Omega_E(t,x,0)}{d(t/T_E)} = -\Lambda(x)\frac{\exp(-t/T_E)}{\sqrt{\pi t/T_E}}. \tag{12}$$

Figures 2(b) and 2(c) show the results of numerical solution of the boundary-value problem describing the decay of horizontal current Ω_E on the surface at various fluid depths. As one can see, the theoretical predictions are in agreement with the numerical results.

Finally, we would like to note that a thin insoluble liquid film covering the fluid surface (e.g., due to contamination [7,25]) can substantially increase the amplitude of the slow current Ω_E^{film} compared to the free surface case, provided that the wave amplitudes remain unchanged, if the compression modulus of the surface film is strong enough. This was demonstrated in Ref. [19] for orthogonal standing waves that generate solenoidal currents with a scale of the order of the wavelength. A similar increase occurs for a large-scale vortex flow as well.

In general, the rheological properties of a thin surface film formed by an insoluble agent can be characterized by four coefficients: dilational elasticity, dilational viscosity, shear elasticity, and shear viscosity [36]. We neglect the internal viscosities of the film and assume that the film is liquid (i.e., the shear elasticity is absent). Then, the film properties can be described solely by the dilational elasticity or the compression modulus $-n(\partial\sigma/\partial n)$, where n is the film surface density and $\sigma(n)$ is the surface tension coefficient. Recently, it has been demonstrated that this simple model describes experimental data fairly well; see Ref. [7].

The wave motion results in periodic contraction and expansion of the fluid surface, which causes periodic deviation of the film density n from its equilibrium value n_0 at the resting surface. Since the surface tension $\sigma(n)$ depends on the surface coverage, it also varies from point to point, giving rise to an additional tangential surface stress, which should be taken into account in the boundary condition for the fluid motion. The effect of a surface film on wave motion and slow induced flow was studied in Ref. [19], and here, based on these results, we calculate (see Appendix D) the enhancement factor for the vertical vorticity Ω_E in the particular case of the wave motion determined by expression (1). The result is

$$\frac{\Omega_E^{\text{film}}}{\Omega_E} = 1 + \frac{\varepsilon^2/\cos^2\theta}{4\sqrt{2}\gamma(\varepsilon^2 - \varepsilon\sqrt{2} + 1)}, \tag{13}$$

where $\varepsilon = \dfrac{-n_0\sigma'(n_0)}{\rho\sqrt{\nu\omega^3}/k^2} \geqslant 0$ is the dimensionless compression modulus of the surface film characterizing its properties at frequency ω and scale $1/k$, and ρ is the fluid mass density. The limiting case of a free surface corresponds to $\varepsilon \to 0$ and in the opposite case $\varepsilon \to \infty$ we deal with an almost incompressible surface film. Note that the presence of a surface film reduces the characteristic time T_S of evolution of the Stokes contribution Ω_S to the vertical vorticity, but does not affect the processes of formation and decay of the Eulerian contribution Ω_E; see Ref. [7]. Therefore, relation (13) is valid for an arbitrary moment of time and for an arbitrary fluid depth $d \gg 1/k$.

To conclude this section, let us discuss the applicability conditions of our approach. The presented theory takes into account only nonlinear terms of the second order in wave amplitudes. All higher-order terms can be neglected, if the effective Reynolds number for the slow current $\mathrm{Re} = \Omega_E \min(T_E, d^2/\nu)$ is small. Note that the fluid viscosity ν enters only in the denominator of the characteristic time of evolution, and this means that the Reynolds number can be reduced by adding glycerol to the water in laboratory experiments [7]. If the value Re is large in the steady-state regime, then the theory can be applied only at the initial stage of evolution, when the value of $\Omega_E t$ remains small.

Although the study focuses on large-scale (compared to the wavelength) vertical vorticity with a characteristic horizontal size $L = 1/(2k\,\sin\theta)$, all steady-state results remain valid for an arbitrary angle 2θ between excited surface waves. The nonstationary analysis implies that the dynamics of the wave amplitudes is much faster than the evolution of the induced Eulerian current. In the case of unbounded fluid with uncontaminated surface, this means that $T_S \ll L^2/\nu$ and it is equivalent to the condition $\theta \ll 1$. However, in laboratory experiments, the friction of waves against the boundaries and the presence of contaminants on the fluid surface can reduce T_S, and then the obtained results remain valid for any angle between the waves as long as the indicated time scales are well separated.

III. CONCLUSION

We demonstrated that surface waves propagating at a small angle to each other generate large-scale solenoidal currents, and we described in detail how they are established and decayed. The obtained results allow for direct experimental verification. If the flow is limited by sidewalls with the size of the order of L, then one should start from the virtual wave stress [18,34] to determine numerically the exact geometry of the induced current, but the qualitative picture remains the same. An important case of the excitation of two crossed standing waves was analyzed in Appendix E. We speculate that large-scale surface currents observed in Refs. [5,7] at large times can be excited due to the mechanism indicated in the paper. The established laws of evolution of large-scale flows will make it possible to test this hypothesis experimentally.

It should also be said that large-scale vortex flows effectively two dimensionalize the system and open the way to the inverse energy cascade, even if the thickness of the system is not small compared to the pumping scale [37]. Probably, such a situation could take place in Refs. [2,3]. Initially, Faraday waves in various directions were excited on the surface and they excited horizontal flows of different scales. Large-scale currents have relatively slow kinetics, and therefore they were not observed shortly after switching on the pumping. In the course of further evolution, their amplitude increased, and they provided an opportunity for the upscale energy transfer.

On the other hand, with a large Reynolds number and a large fluid depth, it is reasonable to expect a picture characteristic of three-dimensional turbulence: a direct energy cascade from large to small scales. Which of these two scenarios is implemented and for which parameters remains unclear. This problem requires further research.

ACKNOWLEDGMENTS

We are grateful to V. Lebedev, I. Kolokolov, and S. Filatov for valuable discussions. This work was supported by the Russian Science Foundation, Grant No. 20-12-00383.

APPENDIX A: STOKES DRIFT CONTRIBUTION TO THE VERTICAL VORTICITY

The calculation of the Stokes drift from the very first principles for an arbitrary wave motion were described, for example, in Ref. [19, Sec. V]. In the case of an uncontaminated fluid surface, the expression for the Stokes drift contribution to the vertical vorticity Ω_S can be written in the form

$$\Omega_S = \epsilon_{\alpha\beta}\left\langle (e^{\hat{k}z}\partial_\beta\partial_t h)(e^{\hat{k}z}\partial_\alpha h)\right\rangle + \epsilon_{\alpha\beta}\left\langle \left(\frac{e^{\hat{k}z}}{\hat{k}}\partial_\beta\partial_\gamma\partial_t h\right)\left(\frac{e^{\hat{k}z}}{\hat{k}}\partial_\alpha\partial_\gamma h\right)\right\rangle. \tag{A1}$$

See [19, Eq. (C3)]. Here $h(t,x,y)$ is the surface elevation due to excited wave motion, $\epsilon_{\alpha\beta}$ is the unit antisymmetric tensor, Greek indices run over x and y, we sum over the repeated indices, $\hat{k} = (-\partial_x^2 - \partial_y^2)^{1/2}$ is the wave-number operator (the square root should be taken with positive real part), and the angle brackets $\langle\cdots\rangle$ mean the averaging over fast wave oscillations. Substitution of the expression

$$h(t,x,y) = H_1\cos(\omega t - kx\,\sin\theta - ky\,\cos\theta) + H_2\cos(\omega t + kx\,\sin\theta - ky\,\cos\theta) \tag{A2}$$

to Eq. (A1) leads to the result

$$\Omega_S = -4H_1H_2\omega k^2\cos^3\theta\,\sin\theta\,\sin[2kx\,\sin\theta]\exp(2kz). \tag{A3}$$

Note also that the Stokes drift produced by the wave motion (A2) was analyzed earlier in the work in [31, Eq. (31)]. The previous result confirms the correctness of the obtained expression.

APPENDIX B: FORMATION OF THE VERTICAL VORTICITY

As it was explained in the main text, the formation of the vertical vorticity Ω_E by surface waves (A2) is described by the following boundary-value problem:

$$\partial_t\Omega_E - \nu\nabla^2\Omega_E = 0, \quad \partial_z\Omega_E|_{z=0} = 2k\,\sin\theta\,\Lambda(x), \quad \Omega_E|_{z=-d} = 0, \tag{B1}$$

where $\Lambda(x) = -4H_1H_2\omega k^2\cos^3\theta\,\sin[2kx\,\sin\theta]$ describes the spatial structure of Ω_E in the horizontal plane. To find the distribution of the vertical vorticity in the vertical direction and its dependence on time during the formation stage, we have to solve the aforementioned boundary-value problem supplemented by a zero initial condition. Performing the Laplace transform for vertical vorticity $\tilde{\Omega}_E(p) = \int_0^\infty d(t/T_E)e^{-pt/T_E}\Omega_E(t)$, where $T_E = L^2/\nu$ and $L = (2k\,\sin\theta)^{-1}$ is the horizontal scale of the current, we find

$$\tilde{\Omega}_E(p,x,z) = \frac{\Lambda(x)}{p\sqrt{p+1}}\frac{\sinh[\sqrt{p+1}(z+d)/L]}{\cosh[\sqrt{p+1}\,d/L]}. \tag{B2}$$

In the inverse Laplace transform, the pole $p = 0$ corresponds to the stationary solution and the points at which $\cosh[\sqrt{p+1}\,d/L] = 0$ form an infinite series describing the evolution to this stationary solution:

$$\Omega_E(t,x,z) = \Lambda(x)\frac{\sinh[(z+d)/L]}{\cosh[d/L]} + \Lambda(x)\sum_{n=0}^{\infty}(-1)^{n+1}\frac{\exp\left[-\frac{t}{T_E}\left(1+\frac{\pi^2L^2(2n+1)^2}{4d^2}\right)\right]}{\frac{d}{2L}\left(1+\frac{\pi^2L^2(2n+1)^2}{4d^2}\right)}\sin\left[\frac{\pi}{2}(2n+1)\left(1+\frac{z}{d}\right)\right]. \tag{B3}$$

The value of the Eulerian contribution to the vertical vorticity on the fluid surface is of particular interest because it is relatively easy to measure experimentally. By substituting $z = 0$ in expression

(B3), one can find

$$\frac{d\Omega_E(t,x,0)}{d(t/T_E)} = \Lambda(x)\frac{L}{d}\exp(-t/T_E)\vartheta_2[0,\exp(-\nu\pi^2 t/d^2)], \tag{B4}$$

where $\vartheta_2[u,q]$ is the Jacobi Theta function. At small times $t \ll d^2/\nu$, the growth of the vertical vorticity on the fluid surface does not depend on the fluid depth d and it is determined by

$$\frac{d\Omega_E(t,x,0)}{d(t/T_E)} = \Lambda(x)\frac{\exp(-t/T_E)}{\sqrt{\pi t/T_E}} \;\Rightarrow\; \Omega_E(t,x,0) = \Lambda(x)\mathrm{erf}\,[\sqrt{t/T_E}]. \tag{B5}$$

At large times $t \gg \min(T_E, d^2/\nu)$, the vertical vorticity on the fluid surface reaches a stationary value determined by the first term in expression (B3). Note that, for a fluid of small thickness $d \ll L$, the stationary solution is reached faster compared with the case of unbounded fluid.

APPENDIX C: DECAY OF THE VERTICAL VORTICITY

In the same way, we can consider the attenuation of the vertical vorticity Ω_E, after the fast decay of the wave motion due to the switching off of the wave maker. In this case one has to solve the boundary-value problem

$$\partial_t\Omega_E - \nu\nabla^2\Omega_E = 0, \quad \partial_z\Omega_E|_{z=0} = 0, \quad \Omega_E|_{z=-d} = 0, \tag{C1}$$

supplemented by the initial condition

$$\Omega_E(0,x,z) = \Lambda(x)\frac{\sinh\,[(z+d)/L]}{\cosh\,[d/L]}, \tag{C2}$$

which corresponds to the time-asymptotic value of expression (B3). The Laplace transform for vertical vorticity is equal to

$$\tilde{\Omega}_E(p,x,z) = \frac{\Lambda(x)\sinh[(d+z)/L]}{p\,\cosh[d/L]} - \frac{\Lambda(x)\sinh[\sqrt{p+1}(z+d)/L]}{p\sqrt{p+1}\,\cosh[\sqrt{p+1}\,d/L]}. \tag{C3}$$

The residue at $p = 0$ is zero and after the inverse Laplace transform we obtain

$$\Omega_E(t,x,z) = \Lambda(x)\sum_{n=0}^{\infty}(-1)^n\frac{\exp\left[-\frac{t}{T_E}\left(1+\frac{\pi^2L^2(2n+1)^2}{4d^2}\right)\right]}{\frac{d}{2L}\left(1+\frac{\pi^2L^2(2n+1)^2}{4d^2}\right)}\sin\left[\frac{\pi}{2}(2n+1)\left(1+\frac{z}{d}\right)\right]. \tag{C4}$$

The term with $n = 0$ determines the asymptotic behavior for large times $t \gg d^2/\nu$. One can also analyze the initial stage of decay of the vertical vorticity on the fluid surface. For small times $t \ll d^2/\nu$, we find

$$\frac{d\Omega_E(t,x,0)}{d(t/T_E)} = -\Lambda(x)\frac{\exp(-t/T_E)}{\sqrt{\pi t/T_E}} \;\Rightarrow\; \Omega_E(t,x,0) = \Lambda(x)\left(\tanh\,(d/L) - \mathrm{erf}[\sqrt{t/T_E}]\right). \tag{C5}$$

APPENDIX D: INFLUENCE OF A THIN INSOLUBLE LIQUID FILM

The influence of the surface film on the slow current Ω_E is substantial if the dimensionless compression modulus $\varepsilon \geqslant 0$ introduced in Ref. [19] is strong enough, $\varepsilon \gg \sqrt{\gamma}$. In the case of monochromatic pumping, the leading terms in the expression for the vertical vorticity are

$$\Omega_E = \hat{\kappa}^{-1}e^{\hat{\kappa}z}\epsilon_{\alpha\beta}\langle 2\partial_\alpha\partial_\gamma h\,k^{-1}\partial_\beta\partial_\gamma\partial_t h + \partial_\alpha h\,\hat{D}\hat{\kappa}\,\partial_t\partial_\beta h\rangle. \tag{D1}$$

See Ref. [19, Eq.(B8)]. In expression (D1) it is assumed that the wave amplitude changes weakly over times of the order of the oscillation period. The angle brackets mean the averaging over the

wave period. The involved operators inside the angle brackets satisfy the following relations:

$$\partial_t = -i\omega = e^{-i\pi/2}\omega, \quad \hat{\kappa} \approx \sqrt{\partial_t/\nu} = \frac{k}{\gamma}e^{-i\pi/4}, \quad \hat{D} = \frac{2i\gamma - \varepsilon}{i\gamma\kappa/k - \varepsilon} \approx 2\gamma\, e^{i\pi/4} + \frac{\varepsilon^2 - e^{-i\pi/4}\varepsilon}{\varepsilon^2 - \sqrt{2}\varepsilon + 1},$$

where operator i shifts the phase of oscillating function by $\pi/2$. Thus the operator presented in the second term in Eq. (D1) is equal to

$$\begin{aligned}\hat{D}\hat{\kappa}\,\partial_t \;&=\; \frac{\omega^{3/2}}{\sqrt{\nu}}\frac{\varepsilon - \varepsilon^2/\sqrt{2}}{\varepsilon^2 - \sqrt{2}\varepsilon + 1} - 2ik\omega - \frac{i\omega^{3/2}}{\sqrt{\nu}}\frac{\varepsilon^2}{\sqrt{2}(\varepsilon^2 - \sqrt{2}\varepsilon + 1)} \\ &\to \left(2k + \frac{\sqrt{\omega}}{\sqrt{\nu}}\frac{\varepsilon^2}{\sqrt{2}(\varepsilon^2 - \sqrt{2}\varepsilon + 1)}\right)\partial_t. \end{aligned} \tag{D2}$$

We kept only the imaginary part of the operator (D2) because the real part is canceled when implementing the summation over $\{\alpha, \beta\}$ in relation (D1). The resulting general expression is

$$\Omega_E = 2k\hat{\kappa}^{-1}e^{\hat{\kappa}z}\epsilon_{\alpha\beta}\left\langle \frac{1}{k^2}\partial_\alpha\partial_\gamma h\,\partial_\beta\partial_\gamma\partial_t h \;+\; \left(1 + \frac{\varepsilon^2}{2\sqrt{2}\gamma(\varepsilon^2 - \sqrt{2}\varepsilon + 1)}\right)\partial_\alpha h\,\partial_t\partial_\beta h\right\rangle. \tag{D3}$$

The accuracy of this expression is that only the leading terms should be kept. They are different depending on the value ε of the film compression modulus. Equation (D3) is formally applicable for the case when the wave amplitude is time dependent varying slowly during one wave period. In the case of two progressive waves (A2), the stationary limit is

$$\Omega_E = e^{2kz\,\sin\theta}\left(1 + \frac{\varepsilon^2/\cos^2\theta}{4\sqrt{2}\gamma(\varepsilon^2 - \varepsilon\sqrt{2} + 1)}\right)\Lambda(x). \tag{D4}$$

APPENDIX E: CURRENTS GENERATED BY STANDING WAVES

The vertical vorticity does not describe the contribution into the slow current which has only horizontal vorticity. This current is excited by a progressive plane wave due to self-nonlinearity [9]. The corresponding velocity on the fluid surface can be estimated as $V_{\text{prog}} \sim \omega d(kH)^2$, where H is the wave amplitude and d is the fluid depth. If the fluid depth d is greater than the horizontal scale L of the vertical vorticity, then the velocity V_{prog} exceeds the velocity associated with the vertical vorticity, $V_{\text{prog}}/V_E \sim d/L$. In the case of standing plane waves, the slow current contribution arising due to self-nonlinearity is absent and the vertical vorticity describes the total slow current.

Let us consider two standing waves excited with some phase shift ψ on the surface of a fluid of infinite depth, i.e.,

$$h(t, x, y) = H_1\cos(\omega t)\cos(kx\,\sin\theta + ky\,\cos\theta) + H_2\cos(\omega t + \psi)\cos(kx\,\sin\theta - ky\,\cos\theta). \tag{E1}$$

Then the Stokes drift contribution into the vertical vorticity is equal to

$$\Omega_S = \omega k^2 H_1 H_2 \sin 2\theta\, e^{2kz}[\sin^2\theta\,\cos(2ky\,\cos\theta) - \cos^2\theta\,\cos(2kx\,\sin\theta)]\sin\psi, \tag{E2}$$

while the Eulerian contribution in the stationary regime is given by

$$\Omega_E = 2\omega k^2 H_1 H_2\,[e^{2kz\,\cos\theta}\sin^3\theta\,\cos(2ky\,\cos\theta) - e^{2kz\,\sin\theta}\cos^3\theta\,\cos(2kx\,\sin\theta)]\sin\psi. \tag{E3}$$

In the last expression in the limit $\theta \ll 1$, the first term is relatively small as θ^3 and localized near the surface, while the second term corresponds to the large-scale current; compare with Eq. (5). Note that the first term produces the correction to the velocity of current which is also relatively small.

Next, if the fluid surface is contaminated by a thin insoluble liquid film with the compression modulus $\varepsilon \gg \sqrt{\gamma}$, then

$$\Omega_E = \frac{\omega k^2 H_1 H_2 \varepsilon^2 \sin\psi}{2\sqrt{2}\gamma(\varepsilon^2 - \varepsilon\sqrt{2} + 1)}[e^{2kz\,\cos\theta}\sin\theta\,\cos(2ky\,\cos\theta) - e^{2kz\,\sin\theta}\cos\theta\,\cos(2kx\,\sin\theta)]. \tag{E4}$$

Compare with Eq. (13). The correction produced by the first term is again relatively small. Thus the general result is that two standing waves (E1) spreading at small angle $2\theta \ll 1$ to each other produce almost straight strips of the current; see text after Eq. (5).

[1] A. von Kameke, F. Huhn, G. Fernández-García, A. P. Muñuzuri, and V. Pérez-Muñuzuri, Double Cascade Turbulence and Richardson Dispersion in a Horizontal Fluid Flow Induced by Faraday Waves, Phys. Rev. Lett. **107**, 074502 (2011).

[2] N. Francois, H. Xia, H. Punzmann, and M. Shats, Inverse Energy Cascade and Emergence of Large Coherent Vortices in Turbulence Driven by Faraday Waves, Phys. Rev. Lett. **110**, 194501 (2013).

[3] N. Francois, H. Xia, H. Punzmann, S. Ramsden, and M. Shats, Three-Dimensional Fluid Motion in Faraday Waves: Creation of Vorticity and Generation of Two-Dimensional Turbulence, Phys. Rev. X **4**, 021021 (2014).

[4] S. V. Filatov, V. M. Parfenyev, S. S. Vergeles, M. Yu. Brazhnikov, A. A. Levchenko, and V. V. Lebedev, Nonlinear Generation of Vorticity by Surface Waves, Phys. Rev. Lett. **116**, 054501 (2016).

[5] S. V. Filatov, S. A. Aliev, A. A. Levchenko, and D. A. Khramov, Generation of vortices by gravity waves on a water surface, JETP Lett. **104**, 702 (2016).

[6] N. Francois, H. Xia, H. Punzmann, P. W. Fontana, and M. Shats, Wave-based liquid-interface metamaterials, Nat. Commun. **8**, 14325 (2017).

[7] V. M. Parfenyev, S. V. Filatov, M. Yu. Brazhnikov, S. S. Vergeles, and A. A. Levchenko, Formation and decay of eddy currents generated by crossed surface waves, Phys. Rev. Fluids **4**, 114701 (2019).

[8] A. P. Abella and M. N. Soriano, Spatio-temporal analysis of surface waves generating octupole vortices in a square domain, JETP **130**, 452 (2020).

[9] M. S. Longuet-Higgins, Mass transport in water waves, Philos. Trans. R. Soc. London A **245**, 535 (1953).

[10] M. S. Longuet-Higgins, A nonlinear mechanism for the generation of sea waves, Proc. R. Soc. London A **311**, 371 (1969).

[11] J. T. Stuart, Double boundary layers in oscillatory viscous flow, J. Fluid Mech. **24**, 673 (1966).

[12] U. Unluata and C. C. Mei, Mass transport in water waves, J. Geophys. Res. **75**, 7611 (1970).

[13] B. D. Dore, On mass transport velocity due to progressive waves, Q. J. Mech. Appl. Math. **30**, 157 (1977).

[14] O. S. Madsen, Mass transport in deep-water waves, J. Phys. Oceanogr. **8**, 1009 (1978).

[15] J. E. Weber, Attenuated wave-induced drift in a viscous rotating ocean, J. Fluid Mech. **137**, 115 (1983).

[16] Z. Xu and A. J. Bowen, Wave-and wind-driven flow in water of finite depth, J. Phys. Oceanogr. **24**, 1850 (1994).

[17] J. E. Weber, Virtual wave stress and mean drift in spatially damped surface waves, J. Geophys. Res.: Oceans **106**, 11653 (2001).

[18] J. A. Nicolás and J. M. Vega, Three-dimensional streaming flows driven by oscillatory boundary layers, Fluid Dyn. Res. **32**, 119 (2003).

[19] V. M. Parfenyev and S. S. Vergeles, Influence of a thin compressible insoluble liquid film on the eddy currents generated by interacting surface waves, Phys. Rev. Fluids **3**, 064702 (2018).

[20] G. Boffetta and R. E. Ecke, Two-dimensional turbulence, Annu. Rev. Fluid Mech. **44**, 427 (2012).

[21] A. Celani, S. Musacchio, and D. Vincenzi, Turbulence in More Than Two and Less Than Three Dimensions, Phys. Rev. Lett. **104**, 184506 (2010).

[22] S. J. Benavides and A. Alexakis, Critical transitions in thin layer turbulence, J. Fluid Mech. **822**, 364 (2017).

[23] R. E. Ecke, From 2D to 3D in fluid turbulence: Unexpected critical transitions, J. Fluid Mech. **828**, 1 (2017).

[24] S. V. Filatov, D. A. Khramov, and A. A. Levchenko, Formation of an energy cascade in a system of vortices on the surface of water, JETP Lett. **106**, 330 (2017).

[25] A. Campagne, R. Hassaini, I. Redor, J. Sommeria, T. Valran, S. Viboud, and N. Mordant, Impact of dissipation on the energy spectrum of experimental turbulence of gravity surface waves, Phys. Rev. Fluids **3**, 044801 (2018).
[26] N. Riley, Steady streaming, Annu. Rev. Fluid Mech. **33**, 43 (2001).
[27] S. Boluriaan and P. J. Morris, Acoustic streaming: from Rayleigh to today, Int. J. Aeroacoust. **2**, 255 (2003).
[28] N. Riley, Oscillatory viscous flows. Review and extension, IMA J. Appl. Math. **3**, 419 (1967).
[29] G. G. Stokes, On the theory of oscillatory waves, Trans. Cambridge Philos. Soc. **8**, 441 (1847) [Reprinted in G. G. Stokes, *Mathematical and Physical Papers* (Cambridge University Press, Cambridge, 1880), Vol. 1, pp. 197–229].
[30] D. Eeltink, A. Armaroli, M. Brunetti, and J. Kasparian, Reconciling different formulations of viscous water waves and their mass conservation, Wave Motion **97**, 102610 (2020).
[31] A. Craik and S. Leibovich, A rational model for Langmuir circulations, J. Fluid Mech. **73**, 401 (1976).
[32] L. D. Landau and E. M. Lifshitz, *Fluid Mechanics*, 2nd ed., Course of Theoretical Physics Vol. 6 (Pergamon Press, Oxford, 1987).
[33] N. Périnet, P. Gutiérrez, H. Urra, N. Mujica, and L. Gordillo, Streaming patterns in Faraday waves, J. Fluid Mech. **819**, 285 (2017).
[34] V. M. Parfenyev and S. S. Vergeles, Virtual wave stress in deep-water crossed surface waves, arXiv:2004.06066.
[35] K. Seshasayanan and B. Gallet, Surface gravity waves propagating in a rotating frame: The Ekman-Stokes instability, Phys. Rev. Fluids **4**, 104802 (2019).
[36] D. Langevin, Rheology of adsorbed surfactant monolayers at fluid surfaces, Annu. Rev. Fluid Mech. **46**, 47 (2014).
[37] H. Xia, D. Byrne, G. Falkovich, and M. Shats, Upscale energy transfer in thick turbulent fluid layers, Nat. Phys. **7**, 321 (2011).